INTERNATIONAL JOURNAL FOR NUMERICAL METHODS IN FLUIDS
Int. J. Numer. Meth. Fluids 2007; **54**:1075–1095
Published online 16 January 2007 in Wiley InterScience (www.interscience.wiley.com). DOI: 10.1002/fld.1415

A proposed modification to the dynamic approach

S. Bhushan*, †

Department of Civil and Environmental Engineering, Duke University, Box 90287, Durham NC-27708, U.S.A.

SUMMARY

In this paper a modification related to the scale-invariancy condition, based on a simple dissipation argument coupled with the hypothesis of Chen *et al.* (*J. Fluids Eng.* 2005; **127**:840–850), is proposed for the dynamic model coefficient evaluation approach. The modification is applied to the Smagorinsky model and used in the calculations of low Reynolds number ($Re_\tau = 180$) channel flow, where the scale-invariancy assumption of the dynamic approach is expected to fail along the wall-normal direction. A detailed analysis of the results is performed for the mean velocity profile, dissipation characteristics, second and higher order statistics, and the energy spectra. The results are compared with the Smagorinsky, the dynamic Smagorinsky, *no model*, the modification proposed by Meneveau and Lund (*Phys. Fluids* 1996; **9**(12):3932–3934), and the DNS data. The proposed modification yields a better model coefficient profile and shows definitive improvement of the results for all flow statistics considered. Copyright © 2007 John Wiley & Sons, Ltd.

Received 26 May 2006; Revised 29 October 2006; Accepted 31 October 2006

KEY WORDS: dynamic approach; channel flow

1. INTRODUCTION

Accurate numerical simulation of turbulent flows requires resolution of a wide range of scales of motion. For complex turbulent flows the range of scales can be large, which makes direct numerical simulation (DNS) infeasible. The alternative approach, which has emerged in the past few decades, is the large Eddy simulation (LES). The philosophy of LES is to capture only the relevant turbulent scales of motion and to model effects of the remaining scales as subgrid stresses (SGSs) [1–4]. Several linear and non-linear models have been proposed for the modelling of SGSs to capture the energy transfer between subgrid and resolved scales of motion accurately [1, 5]. Despite the complexity, all models require specification of model coefficients. Although the coefficients can be evaluated analytically based on canonical theory, these coefficients are seldom found to be universal. In this regard, dynamic evaluation of the model coefficient is one of most important

*Correspondence to: S. Bhushan, Department of Civil and Environmental Engineering, Duke University, Box 90287, Durham NC-27708, U.S.A.
†E-mail: sbhushan@duke.edu

breakthroughs in the SGS modelling. Interested readers are referred to Wang and Bergstorm [6] and others [7–10] for a review on the topic.

The dynamic approach was originally proposed for the Smagorinsky (eddy viscosity) model [7, 11], but since has been applied to several non-linear models [12–15]. The main advantage of the dynamic approach is its capability to adjust the model coefficient in the near wall region and the transition zone [16–19], and thus has been applied successfully to complex engineering problems [1, 19–22]. The dynamic approach, although based on simple physical and mathematical reasoning, involves several open issues such as specification of the filter width ratio [7, 10, 23–25], averaging operation [11, 18], filtering operation [8, 26, 27], and the scale-invariancy assumption [20, 28, 29]. The purpose of this paper is to propose a scale-variancy condition for the dynamic approach coupled with the recent hypothesis of Chen *et al.* [29].

The dynamic approach involves three fundamental assumptions: (1) both the subgrid filter and secondary filter width lie in the inertial subrange; (2) model coefficients are independent of the filtering [6, 8]; and (3) model coefficients at both the subfilter and secondary filter scales are the same (scale-invariance) [19]. The first assumption is associated with the inherent philosophy of the LES and may be violated only if the grid resolution is too coarse. This assumption thus imposes a restriction on the grid resolution (and the secondary filter width) requirement for the LES. The second assumption has been addressed by several researchers such as Ghosal *et al.* [8] and recently by Wang and Bergstrom [6]. However, in the most commonly used version of the dynamic approach, the model coefficient is averaged along the homogeneous direction(s). This eliminates any (spatial) local variations of the model coefficients, thereby satisfying the above assumption. Most critical of these assumptions is the scale-invariancy condition, which fails for the low Reynolds number flows and in the wall region. Meneveau and Lund [28] and Carati and Eijenden [23] reported strong dependence of the dynamic model coefficient on grid resolution for the low Reynolds number isotropic turbulence case. Similar results were also obtained by Wang and Bergstrom [6] for the channel flow simulation. Interested readers are also referred to Porte-Agel *et al.* [20] for more discussion on this issue. To address this drawback Meneveau and Lund [28] obtained an analytic form of the scale-variancy condition following Voke [30]. Porte-Agel *et al.* [20] introduced second test filtering to compute the scale-variancy condition dynamically, which was also adopted by Tejada-Martinez and Jansen [25]. This paper proposes a simple form of the condition based on the dissipation argument. One should expect correct variation of the model coefficient (and proper amount of subgrid stress (SGS) dissipation) along inhomogeneous direction from a scale-variant dynamic model, which is not accounted by the standard dynamic approach.

Apart from the above-mentioned assumptions, the actual implementation of the dynamic approach has also been widely studied. One of the important parameter that has received considerable attention is the optimal filter width ratio [7, 18, 23–25]. Meyers *et al.* [10] suggested the use of a filter width ratio greater than 4, whereas Tejada-Martinez and Jansen [25] introduced dynamic evaluation of the ratio. However, in most of the application [20, 22] the ratio is assumed to be 2, as suggested by Germano *et al.* [7], which is found to be the most robust value. The effect of the filtering and averaging operation has also been studied in detail by several researchers [18, 26–28] both from implementation and stability point of view.

Chen *et al.* [29] (also cf. Bou-Zeid *et al.* [31]) recently provided further insight into the dynamic modelling approach. Their main conclusion, based on the *a priori* test for plane strain flow, is that the model coefficient obtained from the dynamic approach (based on scale-invariancy) correlates well with the coefficients at the test filter scale (of width twice that of filter scale). If the scale-invariance conditions were to hold (such as high Reynolds number isotropic turbulence) then this

DOI: 10.1002/fld

result is of no significance. However, for the low Reynolds number flows or in wall bound flows, the above hypothesis can be coupled with the scale-variancy condition (*a posteriori*[‡]) to obtain the model coefficient. This approach seems more attractive, over the *a priori*[§] approach, as the robustness of the dynamic methodology is retained. Based on the numerical experiments performed here, it was found that the application of the scale-variancy condition *a priori* leads to numerical instability (negative model coefficients) or requires clipping as suggested by Meneveau and Lund [28].

In this paper, Chen *et al.* [29] hypothesis has been coupled with a dissipation-based scale-variancy condition. The details of the formulation are presented in the following section. The approach has been tested for the dynamic Smagorinsky model. Although the linear model suffers from the drawbacks e.g. the stress and strain-rate tensor are parallel [3–5], they remain the most commonly used model for engineering applications [20–22]. Present results thus forms the first step in validation of the approach and can also be easily extended to non-linear models. The first case that has been considered, in Section 3, is the isotropic decaying condition at high Reynolds number, where scale invariancy is expected. This test is important to gain confidence on the dynamic approach and to quantify the divergence from the scale invariancy. This case also provides the contrast for the inhomogeneous flows which is considered next in Section 4, where the model is used in plane channel flow simulation at low Reynolds number ($Re_\tau = 180$). This case represents an ideal case because of the variation of length scale normal to the wall, explicit dependence of the flow on molecular viscosity and availability of the DNS data [32]. The model results have been compared in details with the standard dynamic model, the Smagorinsky model, the *no-model* and Meneveau–Lund [28] scale-variancy relation and the DNS data [32]. The results are summarized and some conclusions are drawn in Section 5.

2. NUMERICAL SIMULATION

The governing equations for LES are obtained by filtering the Navier–Stokes equations, which for the incompressible flows are (cf. Bhushan and Warsi [4] for symbol notation):

$$\begin{aligned} \operatorname{div}\hat{\mathbf{u}} &= 0 \\ \frac{\partial\hat{\mathbf{u}}}{\partial t} + (\hat{\mathbf{u}}\cdot\operatorname{grad})\hat{\mathbf{u}} &= -\operatorname{grad}\hat{p} + \nu\operatorname{div}(\operatorname{grad}\hat{\mathbf{u}}) - \operatorname{div}(\boldsymbol{\tau}) \end{aligned} \tag{1}$$

where $\boldsymbol{\tau} = \widehat{\mathbf{u}\mathbf{u}} - \hat{\mathbf{u}}\hat{\mathbf{u}}$ is the SGS tensor which needs to be modelled. The methodology adopted for modelling the SGS in the present paper is discussed below. For brevity, the models have also been summarized in Table I.

2.1. Smagorinsky model

$$\boldsymbol{\tau} = -2C_s\Delta^2[2\hat{\mathbf{D}}{:}\hat{\mathbf{D}}]^{1/2}\hat{\mathbf{D}} \tag{2}$$

[‡]*A posteriori* coupling of the scale-invariancy condition refers to the approach when the model coefficient is modified after the dynamic model coefficient evaluation.

[§]*A priori* application of the scale-invariancy condition is referred to the approach when the tensor M_{ij} Equation (7) in dynamic approach is modified.

DOI: 10.1002/fld

Table I. SGS model formulation.

Model	
Smagorinsky	$C_s = 0.01$, Δ: Equation (3)
Dynamic model	$C_s\Delta^2$: Equations (7)–(9)
Meneveau	$C_s\Delta^2$: Equations (7), (10) and (9)
Scale invariant (*a priori*)	$C_s\Delta^2$: Equations (7), (11) and (9)
Scale invariant (*a posteriori*)	$C_s^{\tilde{\Delta}}\Delta^2$: Equations (7), (8) and (12); $\frac{C_s^{\tilde{\Delta}}}{C_s^{\Delta}}$: Equation (11)

where Δ is the subgrid filter width which is related to the grid scale, C_s is the suitable value of the model coefficient (assumed constant), and $\mathbf{D}$ is the strain-rate tensor. The filter width is damped close to the wall using the Van-Driest function which yields

$$\Delta = [1 - \exp(-y^+/25)](\delta x \cdot \delta y \cdot \delta z)^{1/3} \tag{3}$$

where δx, δy, and δz are grid sizes in the streamwise, wall-normal, and spanwise directions respectively.

2.2. Dynamic model

The dynamic approach uses the relation between the stresses at two filter levels

$$T_{ij} - \tilde{\tau}_{ij} = L_{ij} = \widetilde{\hat{u}_i \hat{u}_j} - \tilde{\hat{u}}_i \tilde{\hat{u}}_j \tag{4}$$

where the stresses at the secondary filter ($\tilde{\Delta}$) level can be modelled similar to that of the primary filter [7]

$$\mathbf{T} = -2C_s^{\tilde{\Delta}}\tilde{\Delta}^2[2\tilde{\hat{\mathbf{D}}} : \tilde{\hat{\mathbf{D}}}]^{1/2}\tilde{\hat{\mathbf{D}}} \tag{5}$$

The unknown model coefficient C_s can thus be obtained by minimization of the error $(\partial \mathscr{E}^2/\partial C_s)$[11],

$$\mathscr{E} = \mathbf{L} + 2C_s\Delta^2\mathbf{M} \tag{6}$$

where

$$\mathbf{M} = \left(\frac{C_s^{\tilde{\Delta}}}{C_s}\right)\left(\frac{\tilde{\Delta}^2}{\Delta^2}\right)[2\tilde{\hat{\mathbf{D}}} : \tilde{\hat{\mathbf{D}}}]^{1/2}\tilde{\hat{\mathbf{D}}} - \widetilde{[2\hat{\mathbf{D}} : \hat{\mathbf{D}}]^{1/2}\hat{\mathbf{D}}} \tag{7}$$

In the standard dynamic approach scale-invariancy condition is imposed i.e.

$$\frac{C_s^{\tilde{\Delta}}}{C_s} = 1 \tag{8}$$

and the most suitable value of the filter widths is found to be $\tilde{\Delta}/\Delta = 2$. The dynamic model coefficients are hence obtained as

$$C_s\Delta^2 = -\frac{\langle L_{ij}M_{ij}\rangle}{2\langle M_{ij}M_{ij}\rangle} \tag{9}$$

DOI: 10.1002/fld

As evident the dynamic approach does not require external specification of filter width or use of *ad hoc* wall damping function.

2.3. Meneveau and Lund modification

Meneveau and Lund [28] following Voke [30] proposed the following scale-variancy condition:

$$\frac{C_{\mathrm{s}}^{\tilde{\Delta}}}{C_{\mathrm{s}}} = 10^{-3.23[Re_{\tilde{\Delta}}^{-0.92} - Re_{\Delta}^{-0.92}]} \tag{10}$$

where $Re_{\Delta} = \Delta^2 \cdot [2\mathbf{D} : \mathbf{D}]^{1/2}/v$.

2.4. Proposed modification

According to the hypothesis of LES that both the primary and secondary filter widths lie in the inertial subrange, where only energy cascade occurs, the subgrid scale dissipation ($-\boldsymbol{\tau} : \mathbf{D}$) at both the subgrid and secondary filter scales must be equal. This provides the following relation between the model coefficients in lieu of Equation (10):

$$C_{\mathrm{s}}^{\tilde{\Delta}} \tilde{\Delta}^2 \langle [2\tilde{\tilde{\mathbf{D}}} : \tilde{\tilde{\mathbf{D}}}] \rangle^{(3/2)} = C_{\mathrm{s}} \Delta^2 \langle [2\hat{\mathbf{D}} : \hat{\mathbf{D}}] \rangle^{(3/2)} \tag{11}$$

The above scale-variancy relation is actually a numerical counterpart of the Voke's [30] expression or *Meneveau–Lund* [28] curve fitting. Also note that the averaging operator $\langle \cdot \rangle$ and the power has been interchanged [28].

2.5. Chen et al. hypothesis

Recently, Chen *et al.* [29] showed that the dynamic approach provides the model coefficient which correlates much better with the coefficient at the secondary filter width (of size twice that of primary width), i.e.

$$C_{\mathrm{s}}^{\tilde{\Delta}} \Delta^2 = -\frac{\langle L_{ij} M_{ij} \rangle}{2\langle M_{ij} M_{ij} \rangle} \tag{12}$$

The suitable model coefficient at grid scale, C_{s}, is obtained by introducing Equation (12) in the scale-variancy relation, i.e. Equation (11), where the suitable filter width ratios have to be specified.

3. ISOTROPIC DECAYING TURBULENCE

The motivation of these controlled numerical experiments is to compare the analytic model coefficient with that of the dynamic approach and to quantify the divergence from the scale-invariancy condition. For this purpose numerical simulation of the isotropic decaying turbulence based on the experiment of Kang *et al.* [14] is performed, which corresponds to the Reynolds number of 2.472×10^4, at three grid resolutions 32^3, 48^3, and 64^3 (after dealiasing). As the grid scales are large (enough) relative to the dissipation length scale [14], scale-invariancy conditions should hold leading to consistent dynamic model coefficients for all three grid resolutions, and close to analytic value.

DOI: 10.1002/fld

The governing equations are solved using pseudo-spectral methods, using $\frac{3}{2}$-rule for dealiasing [4]. The initial energy spectra was obtained from the experiment [14] (at $x/M=20$) and filtered using Gaussian function [2], which was then superimposed with random phase perturbation [4] for velocity initialization. Because of the sharp-cutoff filtering inherent in the numerical discretization, the resulting primary filter function is a convolution of the Gaussian and sharp-cutoff filter. The primary filter width was thus chosen such that the filter transfer function at cutoff, $G(\kappa_c)$, is 0.8 [25]. This corresponds to $\Delta=1.358\cdot h$, where h is the grid scale. The secondary filter for the dynamic approach was also specified to be Gaussian with width twice of the primary filter, which leads to the filter width ratio $(\tilde{\Delta}/\Delta)^2$ of 5, because of the property of the smooth filter.

To evaluate the Smagorinsky model coefficient we use the isotropic turbulence theory (canonical case) [4], which gives the following relations:

$$\varepsilon = C_s h^2 \langle 2D_{ij} D_{ij}\rangle^{(3/2)} \tag{13}$$

where

$$\langle 2D_{ij} D_{ij}\rangle = 15\left\langle \left(\frac{\partial \hat{u}_1}{\partial x_1}\right)^2 \right\rangle \tag{14}$$

For the given filter function we can estimate,

$$\left\langle \left(\frac{\partial \hat{u}_1}{\partial x_1}\right)^2 \right\rangle = \frac{2}{15}\int_0^{\kappa_c} \kappa^2 \hat{E}(\kappa)\,\mathrm{d}\kappa$$

$$= \frac{12^{2/3}}{h^{4/3}}\left[\Gamma\left(\frac{2}{3};\frac{\pi^2}{12}\right)\frac{C_k}{15}\right]\varepsilon^{2/3} \tag{15}$$

where $\kappa_c=\pi/h$ and the filtered energy spectra, $\hat{E}(\kappa)$, is based on the inertial subrange power law ($\kappa^{-5/3}$). C_k and ε are the Kolmogrov's constant and dissipation, respectively. Interested readers are referred to Bhushan and Warsi [4] for more details of the calculation. This gives the Smagorinsky model coefficient for the filter width Δ to be $C_s=0.0255$. Similarly, the dynamic approach provides the coefficient $C_s\cdot h^2$ which were then modified to $C_s\cdot\Delta^2$. The model coefficients were allowed to evolve and once they reached a quasi-steady state, the simulations were restarted with the velocity field rescaled to the initial energy spectrum.

The energy spectra for the finest grid resolutions are presented in Figure 1, where they compare well with the (filtered) experimental spectra of Kang *et al.* [14] (at $x/M=30$). The results of the constant coefficient Smagorinsky and dynamic models are almost same. Further, the dynamic coefficients in all the three grid resolutions are within $\pm 5\%$ of the Smagorinsky coefficient as shown in Table II. Thus as expected, the dynamic approach works perfectly well when the assumptions of scale-invariancy holds. The proposed scale-variancy function, i.e. $C_s^{\tilde{\Delta}}/C_s^{\Delta}$, was also evaluated *a posteriori* from Equation (11), which showed that for the 48^3 and 64^3 grids the ratio was within $\pm 7\%$ of the scale-invariant value. However, the variation was large (about 27%) for the coarse grid of 32^3. This divergence can be attributed to the fact that the secondary filter width for the coarse grid does not lie in the inertial subrange. The scale-invariant model was used for the finest grid resolution where the results agree well with the dynamic approach.

DOI: 10.1002/fld

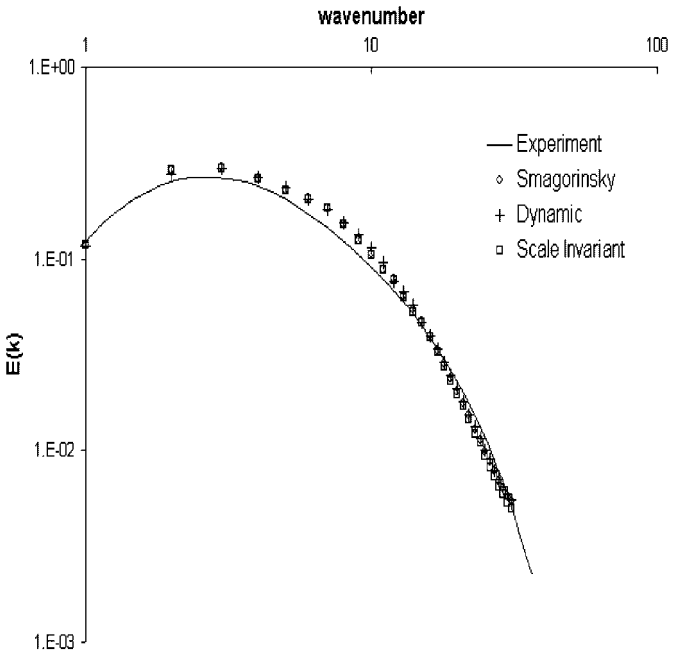

Figure 1. (Filtered) Energy spectra corresponding to $x/M = 30$ in experiment [14] compared with the Smagorinsky, dynamic Smagorinsky, and scale invariant models on 64^3 grid.

Table II. Model coefficients obtained from the dynamic approach and estimate of the deviation from the scale-invariancy condition.

Model	Coefficient (C_s)	% Deviation $\left[\left(1 - \frac{C_s^{\tilde{\Delta}}}{C_s^{\Delta}}\right) * 100\right]$
Smagorinsky	0.0255	—
Dynamic (32^3)	0.0262	+27 %
Dynamic (48^3)	0.0254	+7 %
Dynamic (64^3)	0.0246	−6 %
Scale invariant (64^3)	0.027	+6 %

4. CHANNEL FLOW

The filtered Navier–Stokes equations (Equation (1)) have been solved using pseudo-spectral method, where fast Fourier transform is used in the homogeneous directions (x–z plane) and Chebyshev polynomials in the wall-normal direction (y), and the time stepping is performed using second-order Adams–Bashforth method. Interested readers are referred to Bhushan and Warsi [33] for the details of the numerical scheme. The dimensions of the channel considered for the simulations are same as that of the DNS case [32] ($4\pi \times 2 \times \frac{4}{3}\pi$) along the streamwise ($x$), wall-normal ($y$) and spanwise ($z$) directions, respectively, which is discretized using $32 \times 65 \times 32$ grid points. In the wall-normal directions the grid stretching is controlled by the Gauss–Lobatto points which

DOI: 10.1002/fld

yields fine resolution of $y^+ = 0.21$ close to the wall and $y^+ = 8.83$ in the middle of the channel. The flow is governed by the constant pressure gradient applied along the streamwise direction, which is determined by the Reynolds number of the flow specified to be $Re = 3260$ (equivalent to $Re_\tau = 180.0$ based on half channel width).

The numerical simulations were performed using the constant coefficient ($C_s = 0.01$ [18]) Smagorinsky model (Equations (2) and (3)), standard dynamic model (Equations (7)–(9)), *a priori* scale-variant formulation of dynamic model i.e. Equations (7), (9) and (10) (Meneveau–Lund [28] approach) and Equations (7), (9) and (11) (proposed approach), and the *a posteriori* scale-variant formulation i.e. Equations (12) and (10) (Meneveau–Lund) and Equations (12) and (11) (proposed approach) (cf. table for model formulations). Simulation was also performed without any SGS model referred to as *no-model*, results of which emphasize the effect of SGS modelling.

The results suggest that the stability of the dynamic model is highly dependent on the ratio of the filter width or the factor $F = C_s^{\tilde{\Delta}}/C_s^{\Delta}$ (in Equation (7)) for the scale-variant formulation. The tensor $\mathbf{L}$ was found to be negatively correlated with the rate of strain tensor $\mathbf{D}$ (in an averaged sense), so the positivity of the model coefficient is maintained as long as the tensor $\mathbf{M}$ maintains a positive sign. From Equation (7) we can observe that the first term (without the factor F) on the right is smaller than the second term. Thus, to maintain the positivity the factor F should be larger than 1. Although it is difficult to quantify (locally) the exact minimum value of the factor F, it must be emphasized that the key to the robustness of dynamic model is the specification of factor to 4, as used in engineering applications [20, 22].

In the Meneveau–Lund formulation the ratio (Equation (10)) varied from 1 in the vicinity of the wall to 1.2 in the centre of the channel. This ensured the positivity of the tensor $\mathbf{M}$ and thus of the model coefficient C_s. However, when Equation (11) was used the factor F varied from 1 to 2 (as shown in Figure 3) which leads to negative values of the model coefficients in the sublayer and buffer layer, thereby leading to numerical instability. Experiments were also performed with simple clipping which showed significant improvement of the results over the dynamic model, and the model coefficients were found to be close to the optimum value of 0.01 in the log layer. However, *a posteriori* formulation is preferred as it does not involve any such numerical instability (or *ad hoc* criterion) and provides the best results. *A posteriori* formulation of the Meneveau–Lund approach did not provide significant improvement of the results as the ratio (Equation (10)) was quite small (close to 1) to provide any significant change in the model coefficients. Here, only the key results are presented to emphasize the improvement of the results based on scale-variant formulation. The results referred to as Meneveau–Lund approach are based on the *a priori* formulation, whereas scale-variant approach refers to the proposed formulation applied *a posteriori*. Here the results are presented for the dimensional quantities, as the flow parameters vary significantly for different SGS models (cf. Table III), which tends to obscures the differences between the DNS and the LES results. Whenever the non-dimensionalization is required such as calculation of y^+, DNS data are used.

4.1. Mean flow

The mean streamwise velocity profile (Figure 2) shows that the *no-model* case leads to smaller flow velocity in the log layer. The standard dynamic model improves the result in the correct direction, but still the velocities are less than that of the DNS case. The velocity profile near the wall is well predicted by the dynamic model, whereas the *no-model* overpredicts the velocity slightly. Smagorinsky model on the other hand compares well with the DNS results towards the centre of the channel ($y^+ > 70$). However, close to the wall the excessive dissipation from the model causes

DOI: 10.1002/fld

Table III. Channel flow parameters predicted by subgrid stress models.

Model	τ_{wall}	Re_τ	U_τ^{-1}
DNS	0.002976	178.0	18.33
No-model	0.0032	184.42	17.68
Smagorinsky	0.00273	170.34	19.14
Dynamic	0.00296	177.36	18.38
Scale variant	0.00296	177.56	18.36

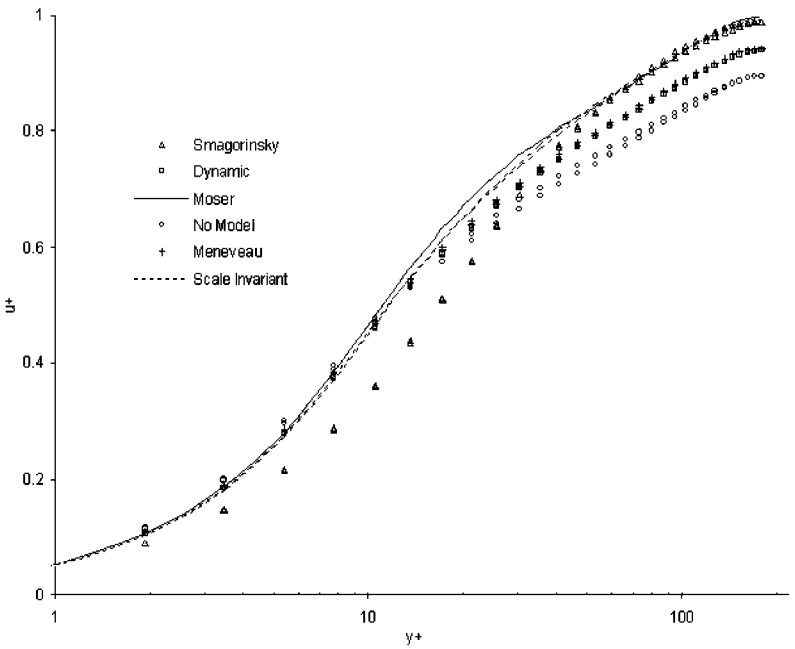

Figure 2. Mean streamwise velocity profiles obtained from different LES runs compared with DNS data.

the velocity profile to deviate from the DNS profile. The *Meneveau–Lund* modification does not provide results much different from the standard dynamic model. The best profile is obtained by the scale-variant model, i.e. Equations (12) and (11) coupled model. The near wall behaviour of the models are best quantified by the wall stress as shown in Table I. Both the scale-variant, dynamic, and *Meneveau–Lund* modification models compares exactly with the DNS values, Smagorinsky model underestimates the stresses and *no-model* overestimates the stresses.

Composite of mean profile and wall stress results suggests that the dynamic model coefficients have correct behaviour in the vicinity of the wall, whereas the Smagorinsky coefficient are correct in the log layer. The dynamic model coefficient profile in Figure 3(a) elucidates the reasons for the discrepancy. As observed the model coefficient compares well with the $y^{+(3/2)}/\Delta^2$ scaling close to the wall, however, in the centre of the channel the coefficient is much smaller (0.004 compared to optimum value of 0.01) away from the wall [18]. The model coefficients obtained from the scale-variant approach has the ideal behaviour as it retains the scaling of the dynamic approach in

DOI: 10.1002/fld

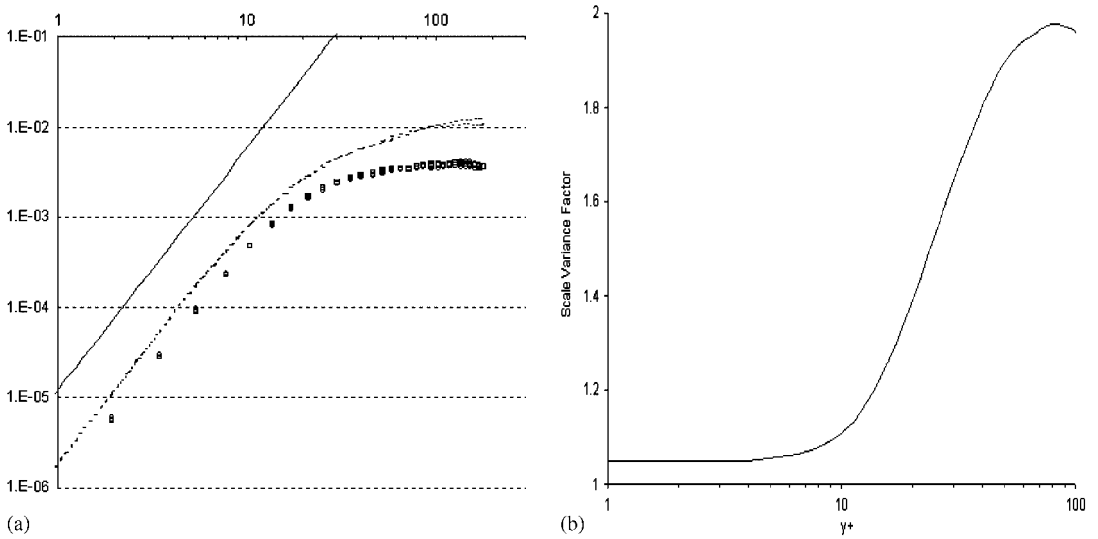

Figure 3. (a) Model coefficient profile, —-: $y^{+(3/2)}/\Delta^2$ scaling; - - - : scale-variant; ○: standard dynamic approach; □: Meneveau–Lund modification; and (b) profile of the factor $F = C_s^{\tilde{\Delta}}/C_s^{\Delta}$ for the scale-variant model, Equation (11).

the sublayer and buffer layer and provides coefficient close to 0.01 in the log layer. The key to this improved coefficient profile is the variation of the factor F along wall-normal direction, shown in Figure 3(b). The factor is 1.05 in the buffer layer, which is close to the expected value of 1.0; as in the near-wall region the turbulent scales are smaller than the grid scales and thus the model coefficient must behave like the Reynolds averaged (RANS) coefficients. The factor transitions smoothly to a stable value of 2.0 in the log layer.

The dissipation profile when compared to the net DNS dissipation (in Figure 4, only the dynamic and scale-invariant model results are presented) shows that the *no-model* overestimates its value close to the wall and underestimates in the buffer and lower-log layer ($50 > y^+ > 10$). Similar behaviour is also observed for the dynamic model. For the Smagorinsky model, the nature is reversed as it overestimates the dissipation in the log layer and underestimates in buffer layer. It must be noted that the total dissipation profile includes the viscous dissipation which is accounts for the mean velocity profile. The SGS dissipation for the Smagorinsky model is of the same order of the viscous dissipation in the log layer, unlike the dynamic model where the SGS dissipation is almost negligible. Scale-invariant model shows an intermediate behaviour of the SGS dissipation and two models and has good agreement with the DNS data in the buffer and lower log layer for the total dissipation.

The subgrid scale dissipation was further decomposed into two components ($\varepsilon^{\mathrm{FS}}$: mean Strain dissipation and $\varepsilon^{\mathrm{FS}}$: redistribution of turbulent kinetic energy within turbulence spectrum) following Hartel and Kleiser [34] and Sagaut *et al.* [35], in order to analyse the backscatter capability of the model. It is expected that the $\varepsilon^{\mathrm{MS}}$ should have negative values in the buffer layer region, however, as seen in Figure 5, the scale-invaraint model is not able of introducing backscatter capability in the dynamic model. This behaviour is expected as the underlining model is the dynamic approach and the model coefficients have been adjusted *a posteriori* to account for accurate amount of net dissipation.

DOI: 10.1002/fld

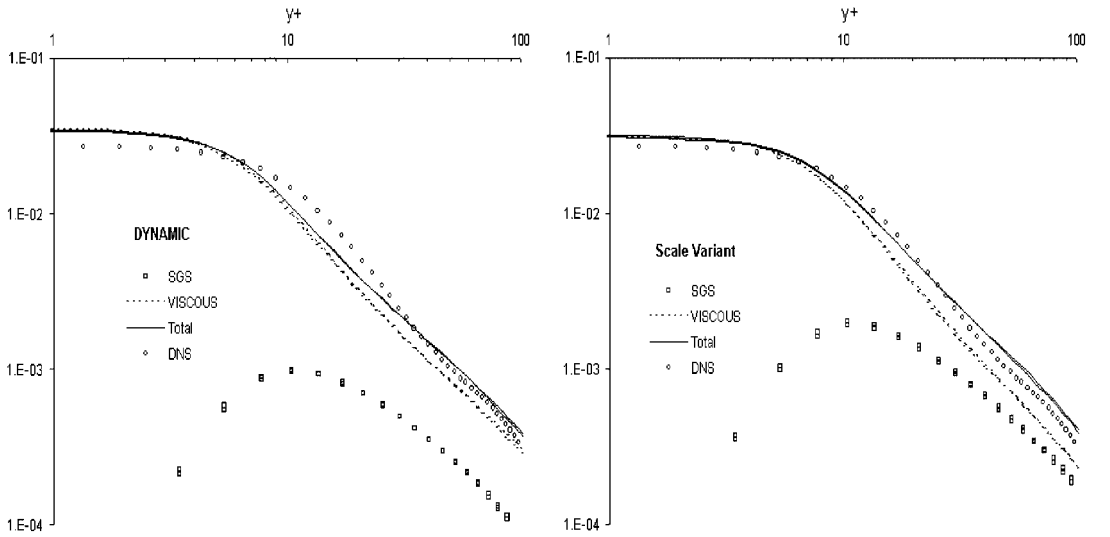

Figure 4. Viscous, SGS and total (SGS + viscous) dissipation profiles from the SGS model runs compared with DNS values: $1/Re(\partial u/\partial y)^2$.

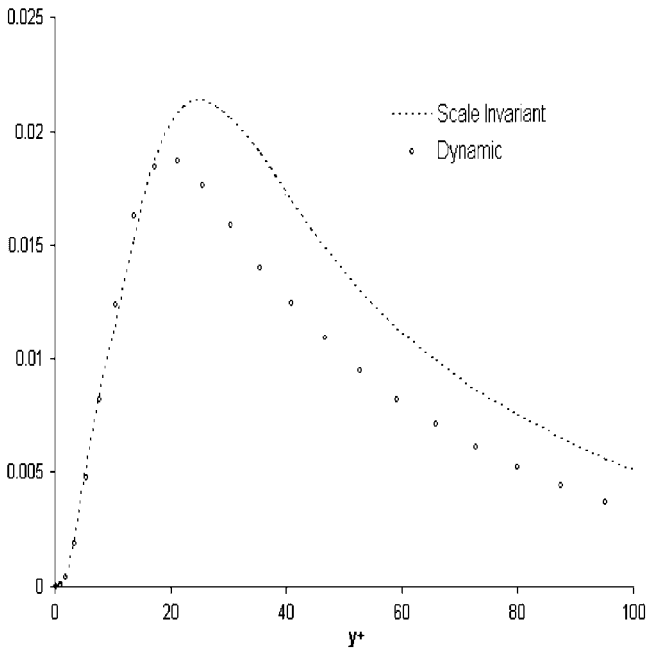

Figure 5. ε^{FS} profile for the dynamic and scale-invariant models. The dissipation has been normalized by u_τ and Re_τ.

DOI: 10.1002/fld

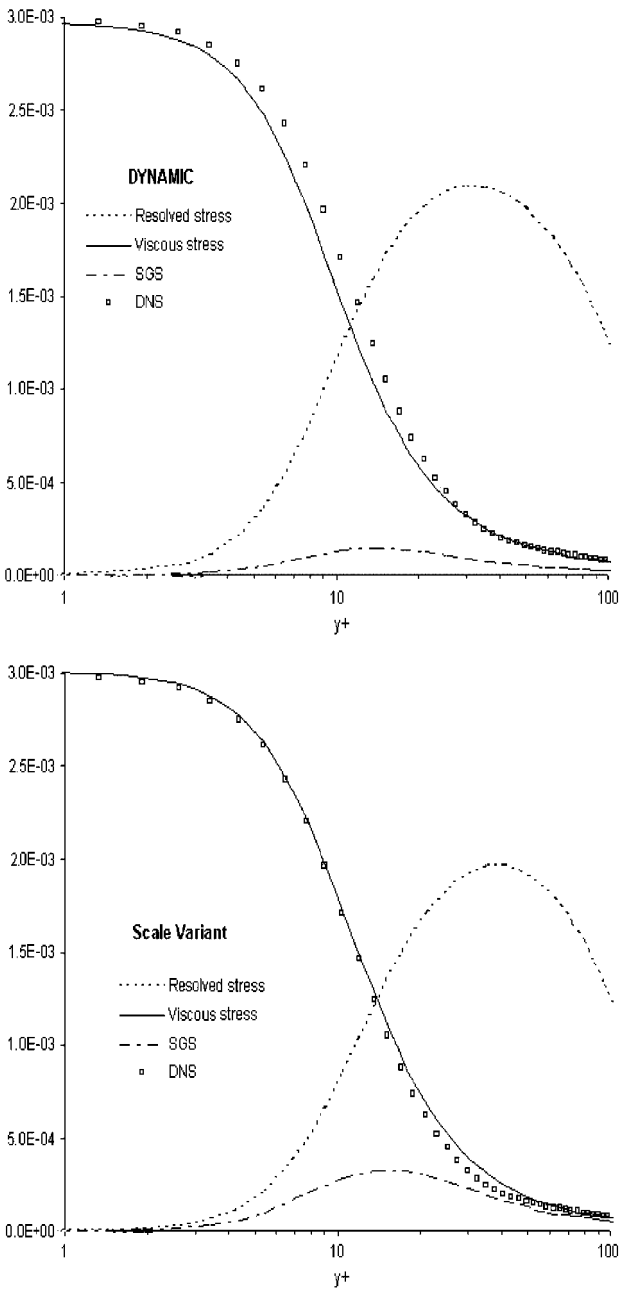

Figure 6. Viscous shear, SGS shear, and resolved shear stress profiles obtained from the LES runs compared with DNS viscous stress profile: $(1/Re)\partial u/\partial y$.

The behaviour of the various models are further emphasized from the shear stress profiles in Figure 6 (only the dynamic and scale-variant results have been shown). *No-model* case has the

DOI: 10.1002/fld

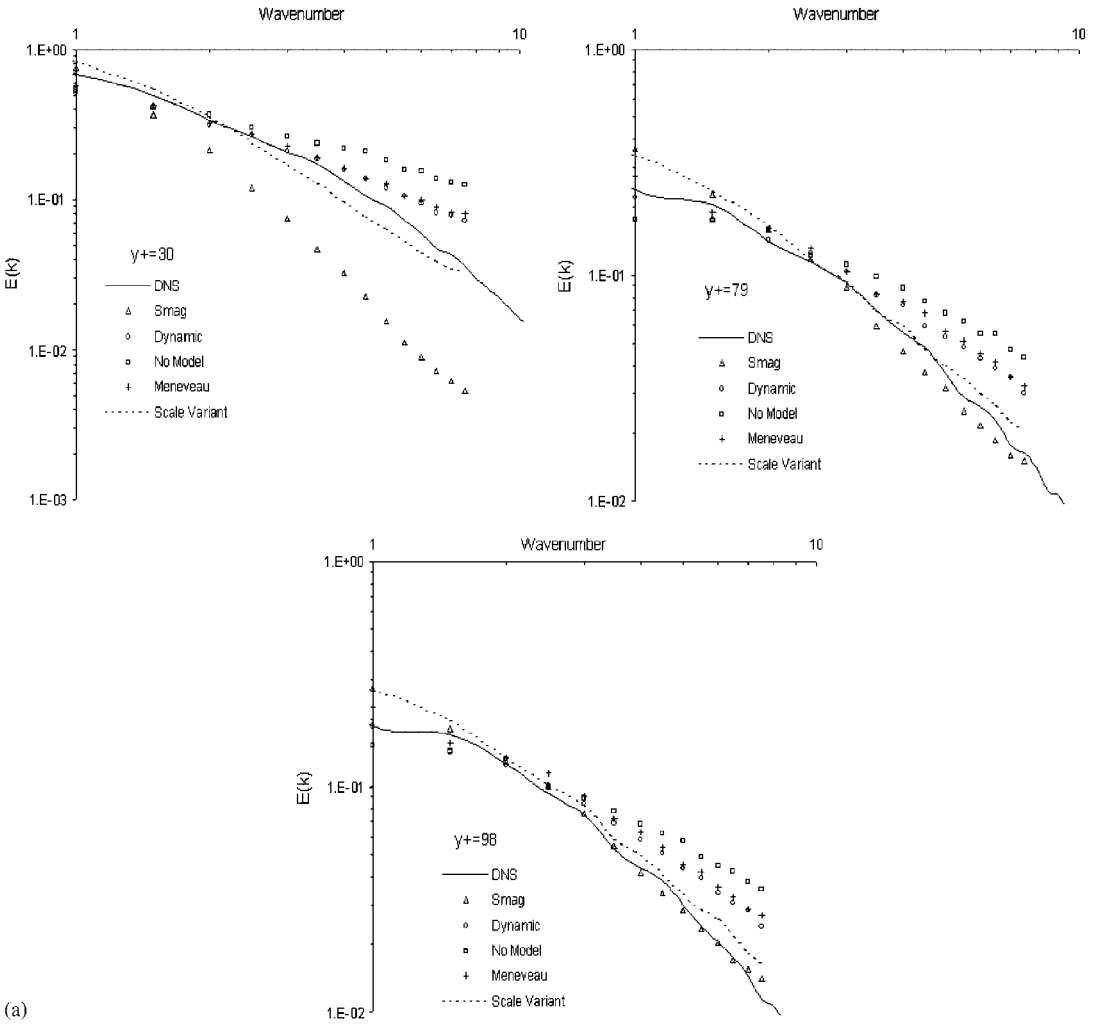

Figure 7. Energy spectra for the: (a) streamwise; (b) wall-normal; and (c) spanwise velocities along the streamwise direction. Results are compared for the different model runs and the DNS data at three locations $y^+ = 30$, 78, and 98.

most resolved stresses followed by the dynamic, the scale-variant, and the Smagorinsky model. The Smagorinsky model shows large SGS stress even in the buffer layer. This component of stress is almost negligible in the dynamic model, whereas the scale-variant model has reasonable profile. On comparison of the viscous stresses with the DNS value, we observe that the *no-model* overestimates the stresses in the sublayer and underestimates in the sublayer and log layer. Similar behaviour is also exhibited by the dynamic model, whereas for the Smagorinsky model the nature is reversed. The scale-variant model is in good agreement with the DNS data in both the sublayer and buffer layer and found best among all the models considered.

DOI: 10.1002/fld

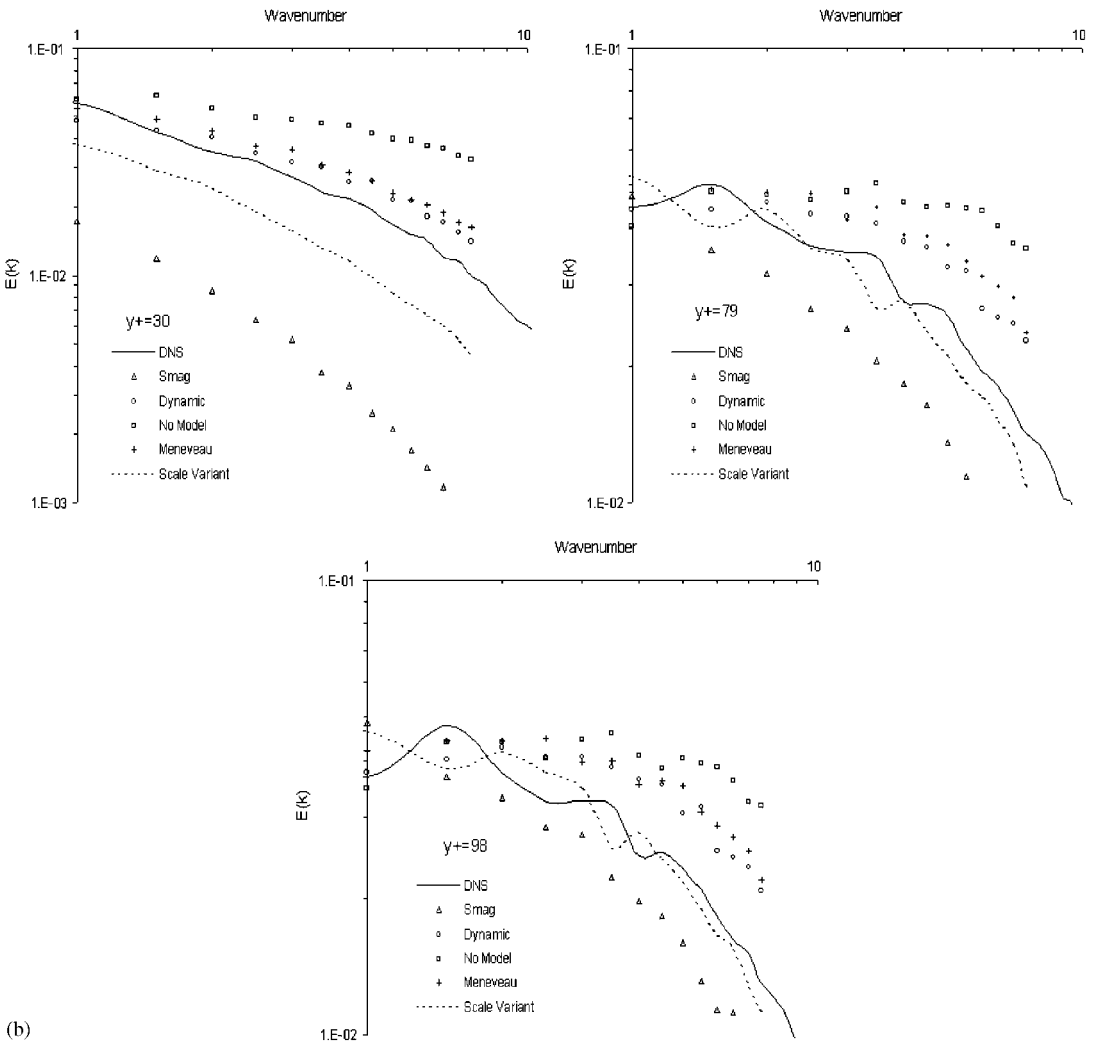

Figure 7. *Continued.*

4.2. Energy spectra

The capability of a LES model to capture the resolved scales of motion can be best depicted by the energy spectra. In Figure 7 the spectra for the velocity correlation along the streamwise direction have been compared with the DNS results. The results have been shown only after the buffer layer, where the turbulence is fully developed. As evident, both the *no-model* and dynamic models overpredict the energy at all the three locations and the velocity components. The *no-model* case overpredicts the energy the most followed by the dynamic model, however, in the buffer layer region these results are better in comparison to the Smagorinsky model which underestimates the energy considerably. The Smagorinsky model is better for the streamwise velocity component for the other two locations $y^+ = 78$ and 98, but not for the spanwise and wall-normal velocity components where

DOI: 10.1002/fld

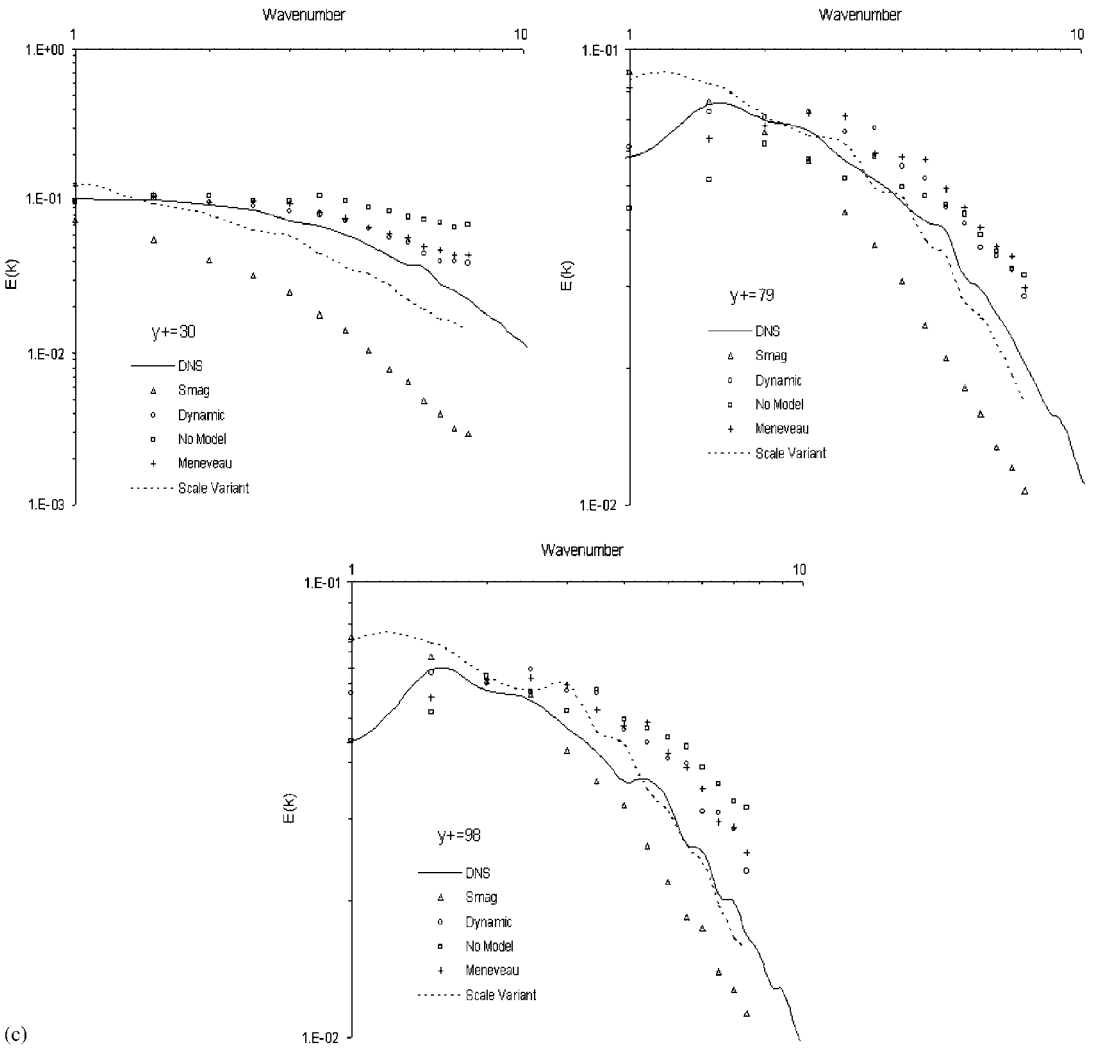

Figure 7. *Continued.*

the energy is underestimated. The scale-variant model is in good agreement with the DNS profile at all the three locations for the streamwise components and in the log-layer region for the other two velocity components. The scale-invariant model, however, underestimates the energy for the wall-normal and spanwise components for the $y^+ = 30$ location.

4.3. Second-order statistics

In Figure 8 the second-order correlations including the shear stress, anisotropic components of u'_{rms}, v'_{rms}, and w'_{rms} have been compared with the DNS data (cf. Bhushan and Warsi [4] for definition of anisotropic components). As seen the *no-model* overestimates the shear stress and the Smagorinsky model underestimates its values and does not capture the peak accurately. The dynamic model

DOI: 10.1002/fld

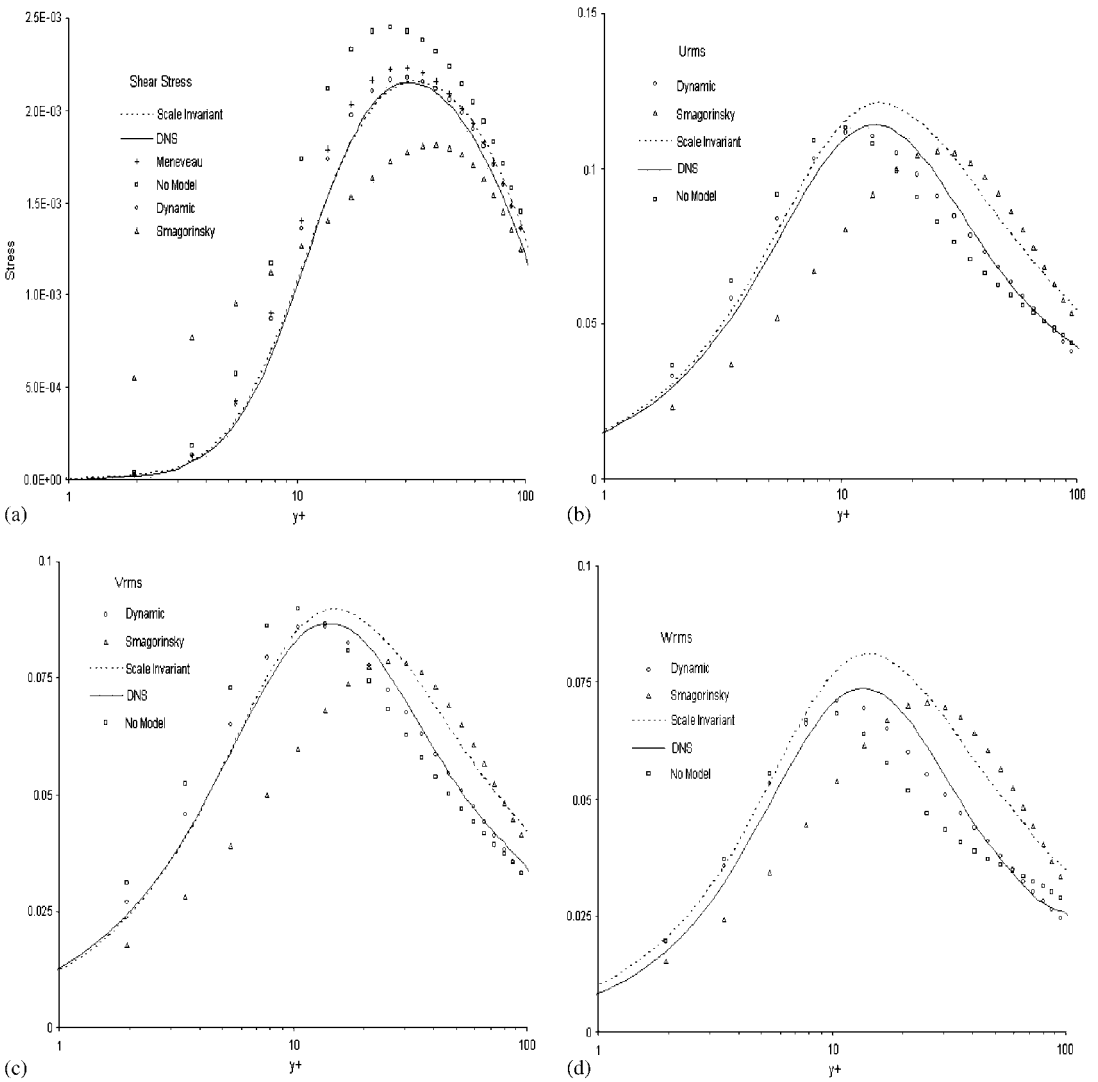

Figure 8. Profile of the second-order statistics: (a) shear stress, anisotropic component; (b) u'_{rms}; (c) v'_{rms}; and (d) w'_{rms} compared with the corresponding DNS values.

and *Meneveau–Lund* modification are in good agreement, however, a perfect match is obtained for the scale-variant model. The (RMS) profile for the streamwise velocity component obtained from both the *no-model* and the dynamic model is almost the same and do not capture the peak very well. The Smagorinsky model does not compare well either and peaks for higher y^+. For the wall-normal and spanwise direction components dynamic model is better than the *no-model* case but again peaks early. The Smagorinsky model fails to capture the profile for these velocity components too. The scale-variant model capture the peaks (for all three velocity components) better than other models, but overestimates the magnitude. The *Meneveau–Lund* modification in these

DOI: 10.1002/fld

cases does not show improvement over the dynamic model and thus corresponding results are not presented.

4.4. Higher-order statistics

In this section the higher-order statistics i.e. the skewness and kurtosis of the velocity fluctuations [4] have been compared with the DNS data in Figures 9 and 10, respectively. For these statistics a perfect agreement between the LES and the DNS data is not expected as the subgrid contributions cannot be estimated. However, assuming that the subgrid scales of motion are more isotropic

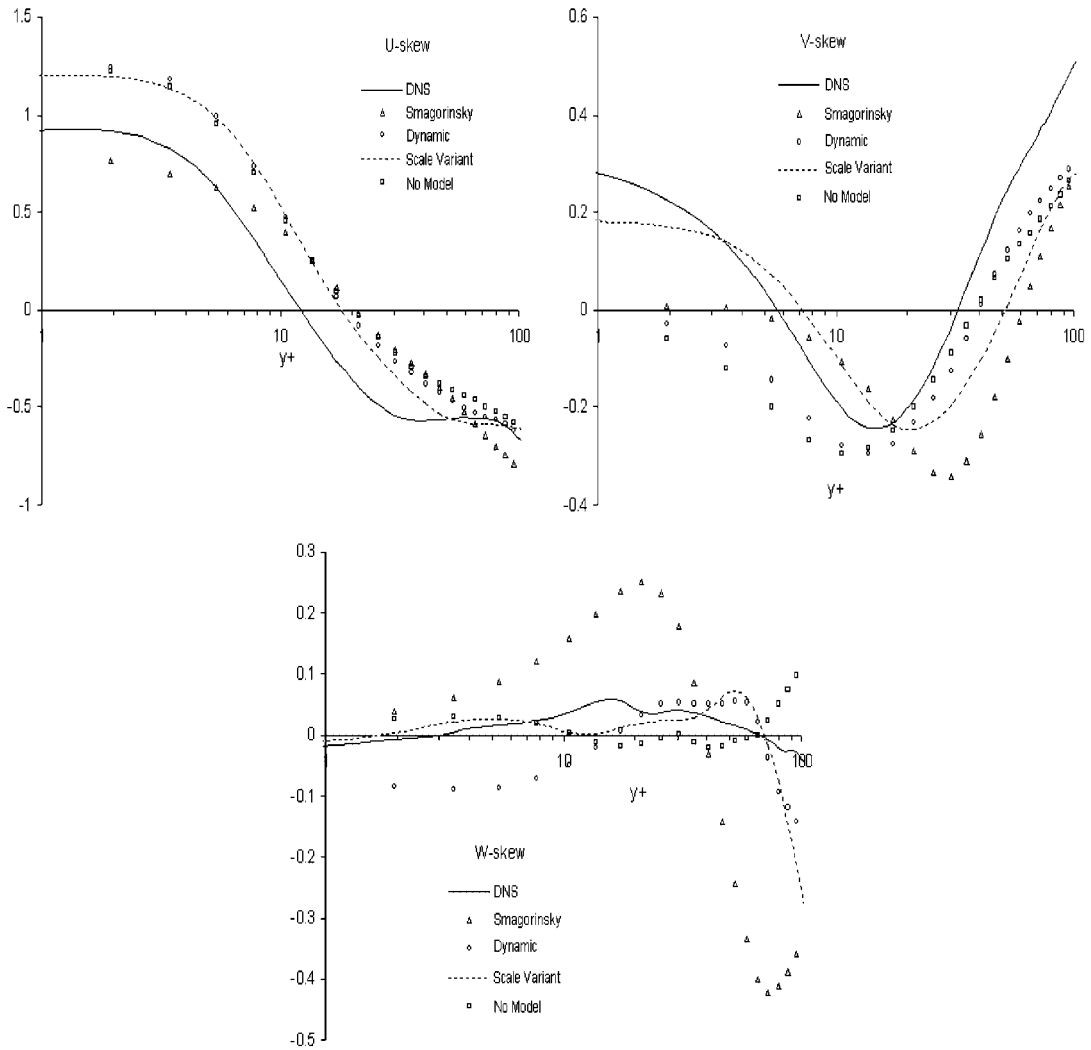

Figure 9. Skewness profile for the streamwise, wall-normal, and spanwise velocity fluctuations as obtained by the LES runs and compared with the DNS data.

DOI: 10.1002/fld

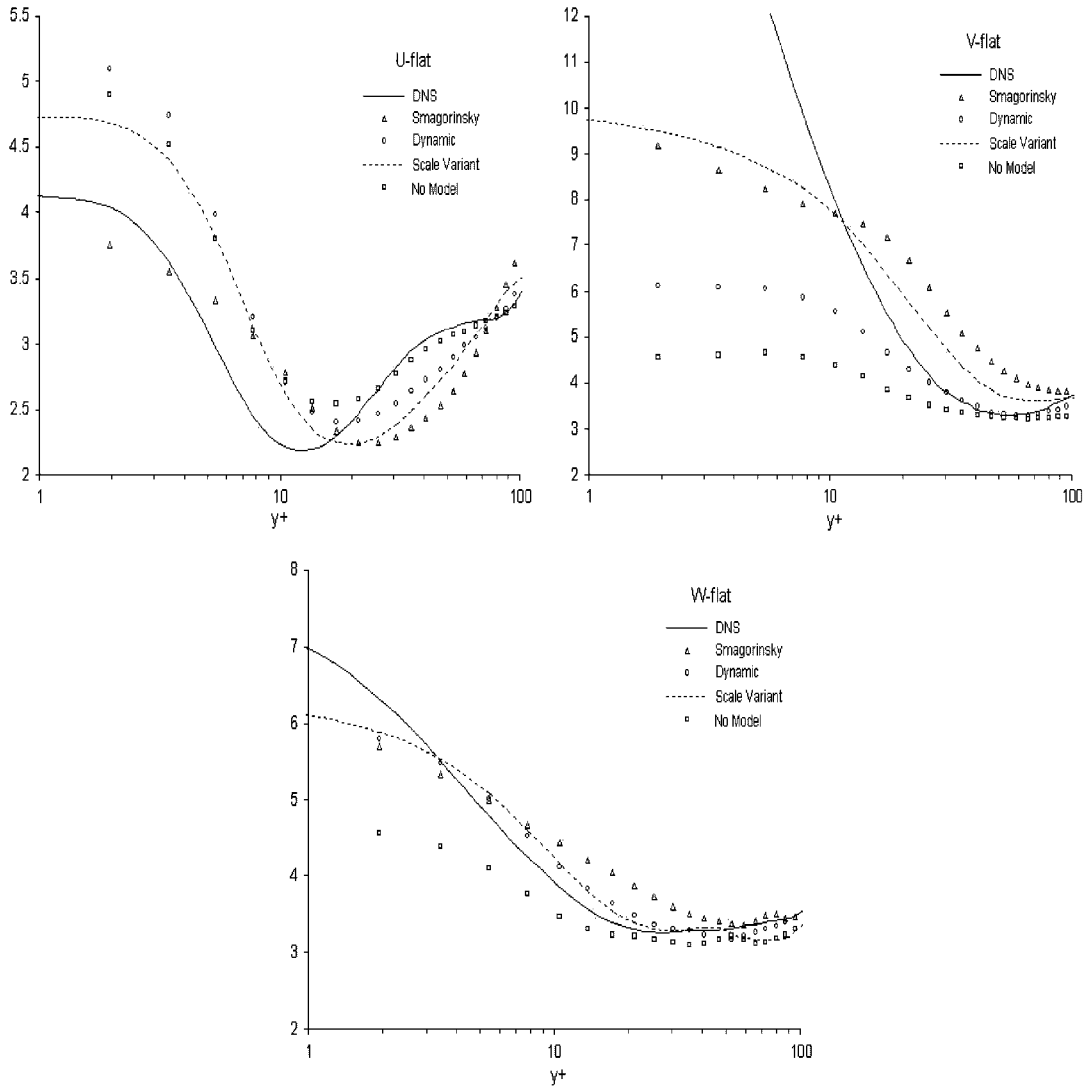

Figure 10. Flatness profile for the streamwise, wall-normal, and spanwise velocity fluctuations as obtained from the LES runs and compared with the DNS data.

and homogeneous in nature, their effect should be to decrease skewness and increase kurtosis. The streamwise velocity fluctuation skewness profile for all the model runs is in good agreement with the DNS data, except for the Smagorinsky model in the near wall region. For the wall-normal velocity component, the scale-variant model performs the best, whereas other models fail to predict the positive skewness in the sublayer region. However, the negative skewness in the buffer layer is depicted by all the models. For the spanwise velocity component, the skewness profile is almost zero because of flow symmetry which is depicted best by the scale-variant and the standard dynamic models.

DOI: 10.1002/fld

The streamwise velocity fluctuation flatness is overpredicted by all the models except the Smagorinsky model, overprediction is least by the scale-variant model. Overall, the nature of the flatness profile is in good agreement with the DNS results except for the Smagorinsky model. The wall-normal velocity flatness diverge near the wall, such divergence is because of the presence of fine scale motions in the DNS, which is not captured in the LES. The scale-variant model leads to maximum flatness followed by the Smagorinsky model. The flatness profile for the *no-model* case does not show significant divergence, whereas the dynamic model peak is too low. For the spanwise velocity components both the scale-variant and the dynamic model results are close to each other and in good agreement with DNS data. Here again, the *no-model* peak is low and Smagorinsky model does not capture the profile.

5. CONCLUSIONS

The dynamic Smagorinsky model has been applied to isotropic decaying turbulence and to a channel flow simulation at low Reynolds number ($Re_\tau = 180$). For the isotropic turbulence case, the dynamic model predicts the model coefficient to be scale invariant (error upto only $\pm 5\%$) as expected. However, for the channel flow, where the scale invariancy is not satisfied along the wall-normal direction, the dynamic model fails to capture the turbulent statistics accurately. The dynamic model was modified by using the (*a priori*) scale-variancy condition, proposed by *Meneveau–Lund* [28], which does not show sufficient improvement in the results. Thus, a new scale-variant formulation based upon a dissipation argument is proposed. Application of the proposed modification leads to correct behaviour of the model coefficient in the log layer but introduces instability in the sublayer and buffer layer. From the numerical experiments it was observed that the best (numerically stable) results are obtained when scale-variancy conditions are applied *a posteriori* coupled with the Chen *et al.* [29] hypothesis. *A posteriori* application of the *Meneveau–Lund* approach did not improve the results in this framework too. However, the proposed modification shows improvement for all flow statistics, such as the mean streamwise flow profile, stress and dissipation profiles, energy spectra, and higher flow statistics. The model coefficient based on the scale-variant dynamic approach shows correct scaling close to the wall and achieves the optimum value of 0.01 in the middle of the channel, where the latter is underestimated by the standard dynamic approach.

The detailed analysis of the channel flow results shows that the scale-variant condition is important for the dynamic approach, and the simple modification proposed here improves the results significantly. The proposed modification still cannot introduce backscatter capability to the dynamic model. In the present paper the scale-variant dynamic approach was applied to the Smagorinsky model, but this method can be also be applied to non-linear models.

It must be noted that the dissipation-based argument put forward in the paper is valid only for the equilibrium turbulence, where subgrid dissipation is constant in inertial subrange. However, for the low Reynolds number channel flow case considered here, the flow does not exhibit such inertial subrange. In the non-equilibrium flows a power law can be assumed for the energy spectrum [36],

$$E(k) \propto k^{\alpha}$$

which Terracol and Sagaut [36], using dimensional analysis of eddy viscosity (cf. Terracol and Sagaut [36] for details), gives the following scaling of the mean SGS dissipation based on

DOI: 10.1002/fld

sharp-cutoff filter width (k_c)

$$\varepsilon(k_c) \propto k_c^{(3\alpha+5)/2}$$

Introducing the following integral in the subgrid scale dissipation formulation:

$$\langle 2\mathbf{D} : \mathbf{D} \rangle = \int_0^{k_c} k^2 E(k)$$

and noting that $k_c = \pi/\Delta$ we obtain

$$C_s^{\Delta} \Delta^2 \langle [2\mathbf{D} : \mathbf{D}] \rangle^{(3/2)} \propto k_{\tilde{\Delta}}^{(3\alpha+5)/2}$$

Thus, the definition of SGS itself should satisfy the correct dissipation scaling for the non-homogeneous case. This also implies scale invariancy of the model coefficient, which is hardly the case. The proposed modification thus provides a mechanism to incorporate the departure from the theoretical scale invariancy. However, in the process dissipation scaling is compromised. Although the proposed modification shows significant improvement in results, inconsistency in the approach can be rectified by using correct dissipation ratio following Terracol and Sagaut [36], for completeness. But would require additional numerical expense associated with another explicit filtering, in order to determine dissipation scaling.

REFERENCES

1. Sagaut P. *Large Eddy Simulation for Incompressible Flows*. Springer: Berlin, 2002.
2. Pope SB. *Turbulent Flows*. Cambridge University Press: Cambridge, 2000.
3. Carati D, Winckelmans GS, Jeanmart H. On the modeling of the subgrid-scale and filtered-scale stress tensors in large-eddy simulation. *Journal of Fluid Mechanics* 2001; **441**:119–138.
4. Bhushan S, Warsi ZUA. Large eddy simulation of turbulent channel flow using an algebraic model. *International Journal for Numerical Methods in Fluids* 2005; **49**(5):489–519.
5. Bhushan S, Warsi ZUA, Walters K. Modeling of energy backscatter via an algebraic subgrid-stress model. *AIAA Journal* 2006; **44**(4):837–847.
6. Wang B-C, Bergstrom DJ. A general optimal formulation for the dynamic Smagorinsky subgrid-scale stress model. *International Journal for Numerical Methods in Fluids* 2005; **49**:1359–1389.
7. Germano M, Piomelli U, Moin P, Cabot W. A dynamic subgrid-scale eddy viscosity model. *Physics of Fluids*, *Series A* 1991; **3**:1760–1765.
8. Ghosal S, Lund TS, Moin P, Akselvoll K. A dynamic localization model for large eddy simulation of turbulent flows. *Journal of Fluid Mechanics* 1995; **286**:229–255.
9. Jimenez J, Moser RD. Large-eddy simulations: where are we and what can we expect? *AIAA Journal* 2000; **38**:605.
10. Meyers J, Geurts BJ, Baelmans M. Optimality of the dynamic procedure for large-eddy simulations. *Physics of Fluids* 2005; **17**:045108:1-9.
11. Lilly DK. A proposed modification of the Germano subgrid-scale closure method. *Physics of Fluids*, *Series A* 1992; **4**(3):633–634.
12. Sarghini F, Piomelli U, Balaras E. Scale-similar models for large eddy simulations. *Physics of Fluids*, *Series A* 1999; **11**(6):1596–1607.
13. Horiuti K. A new dynamic two-parameter mixed model for large-eddy simulation. *Physics of Fluids* 1997; **9**(11):3443–3464.
14. Kang HS, Chester S, Meneveau C. Decaying turbulence in an active grid generated flow and comparisons with large eddy simulation. *Journal of Fluid Mechanics* 2003; **480**:129–160.
15. Zhao H, Mohseni K. A dynamic model for the Lagrangian-averaged Navier–Stokes-α equations. *Physics of Fluids* 2005; **17**:045106:1-10.

DOI: 10.1002/fld

16. Piomelli U. High Reynolds number calculations using the dynamic subgrid scale stress model. *Physics of Fluids*, *Series A* 1993; **5**(6):1484–1490.
17. Piomelli U, Yu Y. Subgrid-scale energy transfer and near-wall turbulence structure. *Physics of Fluids*, *Series A* 1996; **8**(1):215–224.
18. Zhao H, Voke PR. A dynamic subgrid-scale model for low-Reynolds number channel flow. *International Journal for Numerical Methods in Fluids* 1996; **23**:19–27.
19. Meneveau C, Katz J. Scale-invariance and turbulence models for large-eddy simulations. *Annual Review of Fluid Mechanics* 2000; **32**:1–32.
20. Porte-Agel F, Meneveau C, Parlange MB. A scale-dependent dynamic model for large-eddy simulation: application to a neutral atmospheric boundary layer. *Journal of Fluid Mechanics* 2000; **415**:261–284.
21. Ciardi M, Sagaut P, Klien M, Dawes WN. A dynamic finite volume scheme for large-eddy simulation on unstructured grids. *Journal of Computational Physics* 2005; **210**:632–655.
22. Kim HJ, Lee S, Fujisawa N. Computation of unsteady flow aerodynamic noise of NACA0018 airfoil using large-eddy simulation. *International Journal of Heat and Fluid Flow* 2006; **27**:229–242.
23. Carati D, Eijenden EV. On the self-similarity assumption in the dynamic models for large eddy simulations. *Physics of Fluids* 1997; **9**(7):2165–2167.
24. Scotti A, Meneveau C, Lilly DK. Generalized Smagorinsky model for anisotropic grids. *Physics of Fluids*, *Series A* 1993; **5**(9):2306–2308.
25. Tejada-Martinez AE, Jansen KE. A parameter-free dynamic subgrid-scale model for large-eddy simulation. *Computer Methods in Applied Mechanics and Engineering* 2006; **195**:2919–2938.
26. Majander P, Siikonen T. Evaluation of Smagorinsky-based subgrid-scale models in a finite-volume computation. *International Journal for Numerical Methods in Fluids* 2002; **40**:735–774.
27. Wang Y, Jacobitz FG, Rutland CJ. Large eddy simulation of homogeneous shear flows with several subgrid-scale models. *International Journal for Numerical Methods in Fluids* 2006; **50**:863–883.
28. Meneveau C, Lund TS. The dynamic Smagorinsky model and scale-dependent coefficients in the viscous range of turbulence. *Physics of Fluids* 1996; **9**(12):3932–3934.
29. Chen J, Katz J, Meneveau C. Implications of mismatch between stress and strain-rate in turbulence to rapid straining and destraining on dynamic LES models. *Journal of Fluids Engineering* 2005; **127**:840–850.
30. Voke P. Subgrid-scale modeling at low mesh Reynolds number. *Theoretical and Computational Fluid Dynamics* 1996; **8**:131.
31. Bou-Zeid E, Meneveau C, Parlange M. A scale-dependent Lagrangian dynamic model for large eddy simulation of complex turbulent flow. *Physics of Fluids* 2005; **17**:025105.
32. Moser RD, Kim J, Mansour NN. Direct numerical simulation of turbulent channel flow up to $Re_\tau = 590$. *Physics of Fluids* 1999; **11**(4):943–945.
33. Bhushan S, Warsi ZUA. Large eddy simulation of free-shear flows using an algebraic model. *Computers and Fluids*, accepted.
34. Hartel C, Kleiser L. Analysis and modelling of subgrid-scale motions in near-wall turbulence. *Journal of Fluid Mechanics* 1998; **356**:327–352.
35. Sagaut P, Montreuil E, Labbe O, Cambon C. Analysis of the near-wall behaviour of some self-adaptive subgrid -scale models in finite-differenced simulations of channel flow. *International Journal for Numerical Methods in Fluids* 2002; **40**:1275–1302.
36. Terracol M, Sagaut P. A multilevel-based dynamic approach for subgrid-scale modeling in large-eddy simulation. *Physics of Fluids* 2003; **15**(12):3671–3682.

DOI: 10.1002/fld